

Angle-resolved inverse photoelectron spectroscopy studies of CdTe(110), CdS(11 $\bar{2}$ 0), and CdSe(11 $\bar{2}$ 0)

K. O. Magnusson,* U. O. Karlsson,* D. Straub,[†] S. A. Flodström,[‡] and F. J. Himpsel
 IBM Thomas J. Watson Research Center, Box 218, Yorktown Heights, New York 10598

(Received 16 March 1987)

The conduction-band structures of CdTe(110), CdS(11 $\bar{2}$ 0), and CdSe(11 $\bar{2}$ 0) have been studied using angle-resolved inverse photoelectron spectroscopy. With normally incident electrons substantial parts of the conduction bands have been observed and several critical points determined. The energy positions of these are compared with theoretical predictions. Clear discrepancies are found, especially for the wurtzite crystals CdS and CdSe. Unoccupied surface resonances have been observed on CdTe(110) and on CdS(11 $\bar{2}$ 0). Those associated with the broken bonds on the surfaces are found 1.4 and 1.2 eV above the conduction-band minimum (CBM), respectively. On CdS(11 $\bar{2}$ 0) a second surface resonance is found 3.2 eV above the CBM, being split off from the M_1 point in the Brillouin zone. A fluorescence process involving the Cd 4d level has been observed in all three materials. This yields information on the partial density of p states in the valence band.

INTRODUCTION

Investigations of the electronic structure of II-VI compound semiconductors has recently become an area of great activity. The reason for this is the possibility of producing novel materials with adjustable electronic and magnetic properties. Earlier work on II-VI materials is rather sparse. Limiting the scope to the Cd-based subgroup brings us back to the mid 1960s, when interest in the optical properties arose. Experimental work on CdTe (Refs. 1 and 2), CdS, and CdSe (Ref. 3) is noted, together with theoretical bulk-band calculations,⁴⁻⁷ at this time. In 1976 Chelikowsky and Cohen⁸ presented a nonlocal pseudopotential calculations of the bulk bands of, among other crystals, CdTe. This was a consequence of the increased amount of experimental information gained during a decade.⁹ At this time calculations of the surface electronic structure of II-VI compounds began to appear in the literature.¹⁰⁻¹² Low-energy electron diffraction (LEED) studies of the surface geometrical structure had been performed on all three Cd compounds¹³⁻¹⁵ before the first angle-resolved ultraviolet photoelectron spectroscopy (ARUPS) study was made by Ebina *et al.*¹⁶ on ZnSe. The same group has also investigated CdTe,¹⁷ and in 1983 Stoffel¹⁸ presented the first ARUPS study of a wurtzite compound, CdS, using synchrotron radiation. As a consequence of this, a new bulk band calculation for CdS was made by Chang *et al.*,¹⁹ using the local-density approximation (LDA). Recently Magnusson *et al.*²⁰ reported the first observation, using ARUPS, of a surface state on a wurtzite compound semiconductor, CdS.

With the advent of bremsstrahlung spectroscopy the unoccupied electronic states below the vacuum level became accessible through the time-reversed photoemission process, generally called inverse photoemission.^{21,22} Previously these unoccupied states were in some cases observed with other techniques such as photoelectron-yield spectroscopy²³ and electron-energy-loss spectroscopy.²⁴

Optical data on transitions into unoccupied states within a joint density of states formulation were readily available. The interpretation relies in this case on the valence band being known in order to determine the \mathbf{k} -space localization of the transitions. Splittings between critical points in the band structure are accurately determined, but the extended band structure is not obtainable. The large penetration depth of photons in the optical range makes determinations of surface states and resonances difficult.

Inverse photoelectron spectroscopy (IPES) results of conduction-band mappings of Si,²⁵ Ge,²⁶ GaP,²⁷ GaAs,²⁸ and of InP, InAs, and InSb,²⁹ using a spectrometer with a grating monochromator, have been published previously and will in this paper be presented for CdTe, CdS, and CdSe.

EXPERIMENTAL DETAILS

The measurements were performed in an inverse photoelectron spectrometer at IBM, T. J. Watson Research Center, described in detail in Ref. 30. Briefly, the spectrometer consists of a fast $f/4$ grating monochromator with simultaneous detection of the photon spectrum between 8 and 30 eV using two position-sensitive devices. The electrons are emitted from an electron gun in Pierce-type geometry with a low-temperature BaO cathode and impinge under variable angles onto the sample surface. Photons are collected under 45° from the sample surface. Energy and momentum resolutions are typically 0.3 eV and 0.1 Å⁻¹ and are mainly limited by the thermal spread of the electrons. The energy, $h\nu$, of the emitted photon is measured for a chosen initial electron energy E_i . The spectra shown display the measured photon intensity versus the final-state energy E_f which is calculated according to

$$E_f = E_i - h\nu. \quad (1)$$

All final-state energies E_f are measured with respect to

E_F , the Fermi energy of the system. The photon-energy calibration of the analyzer is obtained experimentally from the high-energy cutoff of spectra from evaporated gold films and from the hydrogen Lyman- α radiation.

The samples used were single-crystal rods, $5 \times 5 \times 15$ mm³, of low-resistive CdTe ($\rho \sim 1000$ Ω cm), CdS ($\rho \sim 10$ Ω cm), and CdSe ($\rho \sim 5$ Ω cm) supplied by Cleveland Crystal, Inc. CdTe has the zinc-blende crystal structure and was oriented with the [110] direction coinciding with the 15-mm side of the crystal. Both CdS and CdSe were in the wurtzite phase, oriented with the [11 $\bar{2}$ 0] crystal direction parallel with the 15-mm side. In the indexation of symmetry directions in wurtzite crystals Ref. 20 has been followed. Table I presents the lattice constants and the values of the fundamental energy gap of these Cd II-VI semiconductor compounds.

The crystals were cleaved in an ultrahigh vacuum of better than 10^{-10} Torr and transported under vacuum from the preparation chamber into the measurements chamber, where the pressure never exceeded 5×10^{-11} Torr during the recording of spectra. In the preparation chamber the surface order was checked with LEED and the work functions of the samples were measured using a Kelvin probe. The work function of the probe was calibrated against cleaved Si(111) surfaces which have a very reproducible work function of 4.85 eV, almost independent of doping and cleavage quality.³¹

Ohmic contacts were alloyed onto the sample using a gallium-aluminum alloy, to avoid uncontrolled voltage drops at the sample-sample-holder interface. These contacts were checked prior to the experiment by I - V measurements. To further check the quality of this procedure spectra were recorded after evaporation of Ti onto the cleaved surface. In these spectra the Fermi edge is visible and any shift in its position relative to the final-state energy, $E_f=0$, would be an indication of charging. No shifts were observed.

Several cleaves of varying quality were made on the crystals. All spectra presented in this paper are from visually smooth surfaces except in the case of CdSe, to be discussed later.

RESULTS AND DISCUSSION

CdTe(110)

Figure 1 shows recorded distributions of photons emitted through the inverse photoemission process from the (110) cleavage face of CdTe. The electrons are impinging on the crystal surface at normal incidence with a kinetic energy of E_i , relative to the Fermi energy E_F of

the crystal. The valence-band maximum (VBM) relative to E_F is found using the relation

$$E_F - E_{\text{VBM}} = \phi_\theta - \Phi, \quad (2)$$

where the photothreshold $\phi_\theta = 6.2$ eV (Ref. 32) and Φ , the work function, was measured to be 4.86 eV giving the position of the VBM at 1.34 eV below E_F . The band gap of $E_g = 1.59$ eV gives the conduction-band minimum (CBM) at 0.25 eV above E_F (see also Table I).

In the spectra, three regions of strong emission intensity will be discussed. Around 2 eV above E_F we observe the overall strongest feature, which at $E_i = 12.25$ eV has a full width at half maximum (FWHM) of 1.7 eV, being centered at 2.4 eV above E_F . This peak can be easily followed through the series in E_i and strong changes in its shape can be observed. At a kinetic energy of the exciting electrons of 16.25 eV this peak has sharpened up considerably; the FWHM is 1.0 eV, but with a strong shoulder contribution on the low-photon-energy side. When we reach $E_i = 18.25$ eV a drastic reduction in intensity is observed and at higher E_i this peak becomes weak.

The second photon-energy region of importance is in the neighborhood of 5 eV. The structures appearing here can be studied with $E_i > 14$ eV. When E_i is increased the two peaks merge into each other and one sharp, intense peak is observed for $E_i = 18.25$ eV. For higher E_i this peak broadens.

The third interesting contribution to the spectra becomes visible first when the kinetic energy of the electrons reaches 16.25 eV. In this spectrum a broad peak, marked with an arrow, is found at 7.0 eV above E_F . With $E_i = 17.25$ eV the peak is found not at 7.0 eV but at 8.0 eV above E_F and this pattern is followed throughout the series.

The theory within which we want to interpret these results is the model of momentum-conserving direct transitions, where the electrons emitted from the gun pass the solid-vacuum interface conserving the momentum parallel with the interface, k_{\parallel} , except for a possible surface umklapp with a surface reciprocal-lattice vector \mathbf{G}_{hk} . The electrons will then fill normally unoccupied states from which a direct transition into an unoccupied state of lower energy can take place. Also in this process there is the possibility of an umklapp event, here with a bulk reciprocal-lattice vector \mathbf{G}_{hkl} . With $k_{\parallel} = 0$ transitions along the Γ -(K)- X line in the Brillouin zone are excited.

One problem in making an interpretation with the aim to map the conduction band is finding the initial state of

TABLE I. Summary of available geometric and electronic data on CdTe, CdS, and CdSe. Presented are the lattice constants a and c , the value of the fundamental band gap E_g , reported photothresholds ϕ_θ , and the measured work function Φ .

	a (Å)	c (Å)	E_g (eV)	ϕ_θ (eV)	Φ (eV)	$E_F - E_{\text{VBM}}$ (eV)
CdTe	6.48		1.59	6.2 ^a	4.86	1.34
CdS	4.13	6.70	2.58	7.2 ^a	4.79	2.41
CdSe	4.30	7.02	1.98	6.6 ^a	5.35	1.25

^aReference 32.

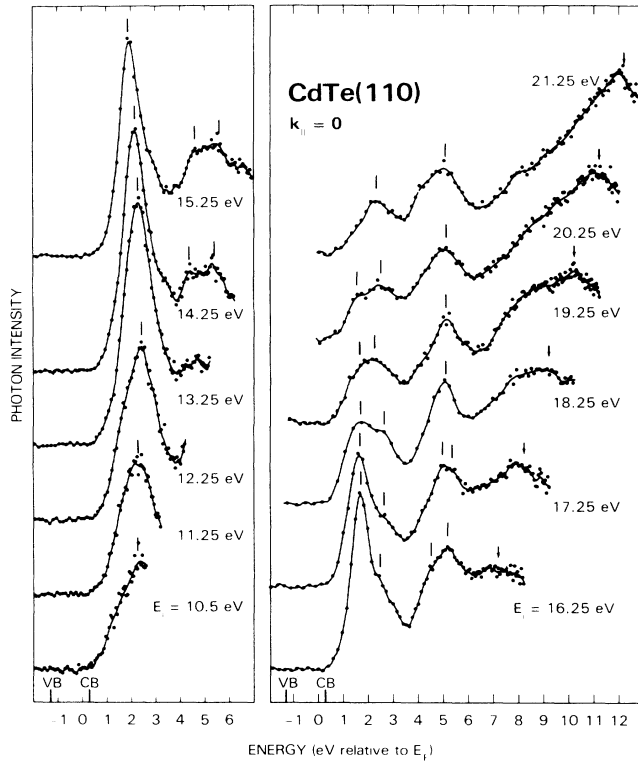


FIG. 1. Inverse photoemission spectra recorded for different kinetic energies E_i of the electrons impinging at normal incidence, $k_{\parallel}=0$, on the cleaved (110) surface of CdTe.

the transitions and thus being able to deduce the momentum perpendicular to the surface. Outside the solid the electron is in a free-electron state. A common assumption for electronic states involved in electron emission and, as in this case, electron absorption processes, when these states lie sufficiently high in energy (relative to, e.g., E_F), is that they are free-electron-like.^{18,28} Explanations of any discrepancies found can then, under favorable circumstances, be based on the calculated bands in this energy region. In this paper the initial state will be assumed to be free-electron-like, described by the parabolic equation

$$E_i = (\hbar^2/2m_e)(\mathbf{k} + \mathbf{G}_{hkl})^2 + E_0, \quad (3)$$

where \mathbf{G}_{hkl} is a reciprocal-lattice vector and E_0 is the inner potential with respect to the VBM. We have used a value for the inner potential of $E_0 = -5.0$ eV. This value has been used to interpret photoelectron-spectroscopy results.³³ No calculated bands are available in the relevant initial-state energy range.

The two peaks in the structure around 5-eV final-state energy in Fig. 1 are found to originate from direct transitions between the $\mathbf{G} = (-2, -2, 0)$ free-electron initial band and the conduction bands approaching the Γ_7 and Γ_8 points. These experimental points have been marked with circles in Fig. 2, where also the initial bands used and the calculated bands from Chadi *et al.*⁷ are shown. The energy reference is here and in all $E(\mathbf{k})$ dispersion graphs, taken as the VBM in order to compare with cal-

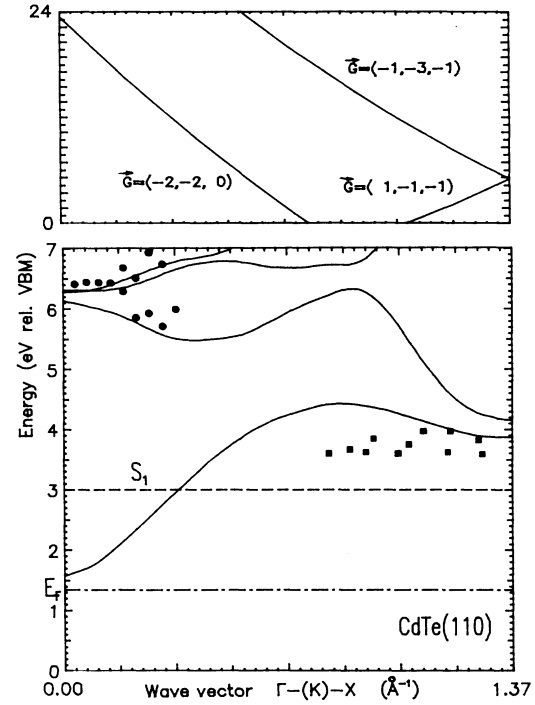


FIG. 2. Final state energies E_f , relative to the VBM, of the transitions observed on CdTe(110) plotted vs k_{\perp} determined assuming the initial state to be free-electron-like. The upper panel shows the initial states involved, labeled with the relevant reciprocal-lattice vector \mathbf{G} . Transitions from the $\mathbf{G} = (-2, -2, 0)$ are marked with circles, while squares denote transitions from the $\mathbf{G} = (-1, -1, -1)$ or $(-1, -3, -1)$ initial state. The dashed line indicates the energy position of the Cd-derived through contamination-dependent measurements. The solid lines are the calculated conduction bands from Chadi *et al.* (Ref. 7). The dashed-dotted line is the Fermi level.

culations. The Γ_8 critical point is found at 6.4 eV above the VBM.

The structure at 2 eV above E_F in Fig. 1 is somewhat more complicated. First we note that it is a double-peak structure. This is clearly seen in the $E_i = 16.25$ -eV spectrum. At lower E_i (e.g., 11.25 eV) the dominating structure is the one corresponding to the transition which shows up as the shoulder in the 16.25-eV spectrum. As E_i is increased, the structure on the high-photon-energy side (closer to E_F) increases in intensity until we reach $E_i = 16.25$ eV where it starts decreasing again. With no conduction band states 3.3 eV above the VBM close to Γ in the Brillouin zone, the $\mathbf{G} = (-2, -2, 0)$ bands are excluded as initial states for the above-discussed double structure.

In Fig. 3 the $E_i = 16.25$ -eV spectrum is shown together with a spectrum from a contaminated sample and a spectrum from a poor cleave. When the spectra are subtracted a distinct peak at 1.6 eV above E_F is observed. The conclusion is that part of the peak dominating the 16.25-eV spectrum is due to transitions into an unoccupied surface resonance on the CdTe(110) surface, lying 1.4 eV above the CBM at $k_{\parallel} = 0$. (With a surface resonance we mean an electronic state localized to the sur-

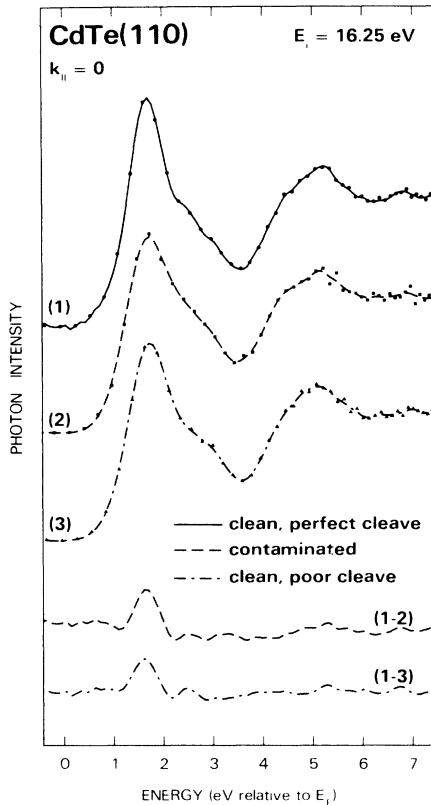


FIG. 3. Inverse photoemission spectra from CdTe(110) recorded at normal incidence, $k_{\parallel}=0$, with $E_i=16.25$ eV. The top spectrum (1) is from a fresh cleave, the middle spectrum (2) is from the same cleave but recorded after 12 hours of exposure of the surface to the electron beam, and curve (3) is from a clean but poor cleave. Below these are shown the difference spectra between (1) and (2) and between (1) and (3).

face, being two-dimensional in \mathbf{k} , but having overlap in energy with bulk electronic states.) The second structure, which shows up as a shoulder in the 16.25-eV spectrum, is due to direct transitions into the lowest conduction band in the neighborhood of X_6 . We find satisfactory consistency with the calculated conduction bands assuming that the initial state also here is free-electron-like, but using a reciprocal-lattice vector $\mathbf{G}=(1, -1, -1)$, $(-1, -3, -1)$. In Fig. 2 the surface resonance is marked with a dashed line and the experimental points belonging to transitions into the lowest conduction band are marked with squares. The X_6 critical point is found at 3.7 eV above the VBM.

The peak which is found at 8.0 eV above E_F in the $E_i=17.25$ -eV spectrum in Fig. 1, "dispersing" in final-state energy in pace with the change in electron kinetic energy, has its origin in a fluorescence process involving the Cd 4d state. For this reason it is not indicated in Fig. 2. When the incident electron carries enough kinetic energy to excite the Cd 4d electron into an unoccupied state (at $E_i=17.25$ eV even enough to initiate an emission process), a hole is left in the Cd 4d level, in the first approximation with equal probability throughout

the first Brillouin zone. This hole will be filled by a transition from the valence band, with the subsequent emission of a photon carrying the energy difference. The maximum in photon intensity will be found at the photon energy corresponding to the energy difference between the maximum in the valence partial density of states of p -character and the Cd 4d state, as a consequence of dipole selection rules. The transition at 8.0 eV in the $E_i=17.25$ eV spectrum corresponds to a photon energy of $h\nu=17.25-8.0=9.25$ eV. With the weighted average binding energy of the Cd 4d level of -9.40 eV,³³ this puts the maximum of the valence partial density of p states 0.15 eV below the VBM.

CdS(11 $\bar{2}$ 0)

Using Eq. (2) with a phototreshold $\phi_{\theta}=7.2$ eV (Ref. 32) and the measured work function $\Phi=4.79$ eV, the Fermi energy is found at 2.41 eV above the valence-band maximum. With the energy gap of 2.58 eV this puts the conduction-band minimum of 0.17 eV above E_F .

Figure 4 shows a series of normal-incidence inverse photoemission spectra recorded from the cleaved (11 $\bar{2}$ 0) face of CdS. Five different contributions labeled A, B, C, D, and E will be discussed. In addition to these, a sixth structure appears for $E_i \geq 18.25$ eV at a constant photon energy of $h\nu=9.25$ eV. This structure has been marked with an arrow in the $E_i=21.25$ -eV spectrum. The structures C, D, and E can be followed unambiguously throughout the series from the kinetic energy at which they first appear. No drastic changes in intensity

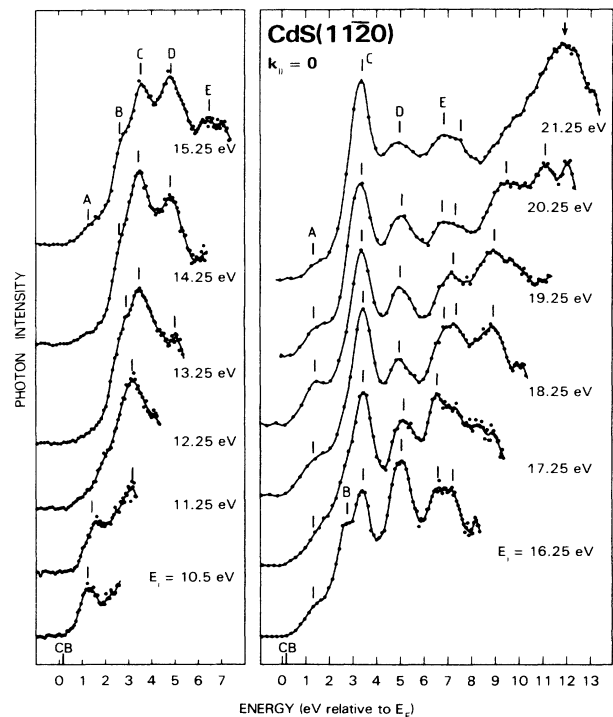


FIG. 4. Inverse photoemission spectra recorded for different kinetic energies E_i of the electrons impinging at normal incidence, $k_{\parallel}=0$, on the cleaved (11 $\bar{2}$ 0) surface of CdS.

are noticed and the most obvious dispersion is found in *C*, having a 0.4-eV dispersion. The structure labeled *B* appears as a distinct shoulder in four spectra. In most every spectrum a contribution on the high-photon energy side (closest to E_f) can be observed. This structure, labeled *A*, is clearly resolved as a peak in the $E_i = 19.25$ -eV spectrum and even more in the $E_i = 10.5$ -eV and 11.25-eV spectra.

In Fig. 5 the contamination and cleavage dependence of the structures can be studied. For $E_i = 19.25$ eV, spectra from a clean and a contaminated sample, both recorded from a good cleave, are presented together with a spectrum from a poor cleave. Difference spectra between the clean and contaminated sample and between the good and poor cleave at $E_i = 19.25$ eV are also shown.

The interpretation of the results presented above is made within the model of direct transitions assuming the initial state to be well approximated by a free-electron

parabolic state, as discussed previously. In angle-resolved photoelectron spectroscopy work on CdS, Magnusson³³ has used a single free-electron final-state band with an inner potential $E_0 = -3.5$ eV relative to the VBM. This is also in fair agreement with the results of Stoffel.¹⁸ In Fig. 6 the calculated lowest conduction bands from Chang *et al.*¹⁹ are presented together with the experimental points found using the free-electron initial bands with $\mathbf{G} = (1,1,-2,0)$, $(-2,-2,4,0)$ and the photoelectron-spectroscopy-derived value of the inner potential. The calculated conduction bands have been rigidly shifted to give the correct band gap of CdS.

The structure *D* is found to be due to transitions into the conduction band approaching the M_4 point. The M_4 critical point is found at 7.5 eV above the VBM. For the peak *E*, found around 7.0-eV final-state energy in Fig. 4, no calculated band has been available, but the assumption that this is due to direct transitions into a conduction band in this region seems probable. The two lowest conduction bands are observed in this study as the contributions *B* and *C*. The structure *C* can be followed throughout the series. The experimental points in Fig. 6 associated with the structure *C* form a band, the shape of which agrees well with the calculated second-lowest conduction band, but the absolute energy position in the region where transitions are observed is underestimated by ~ 0.7 eV. The conclusion is supported by the

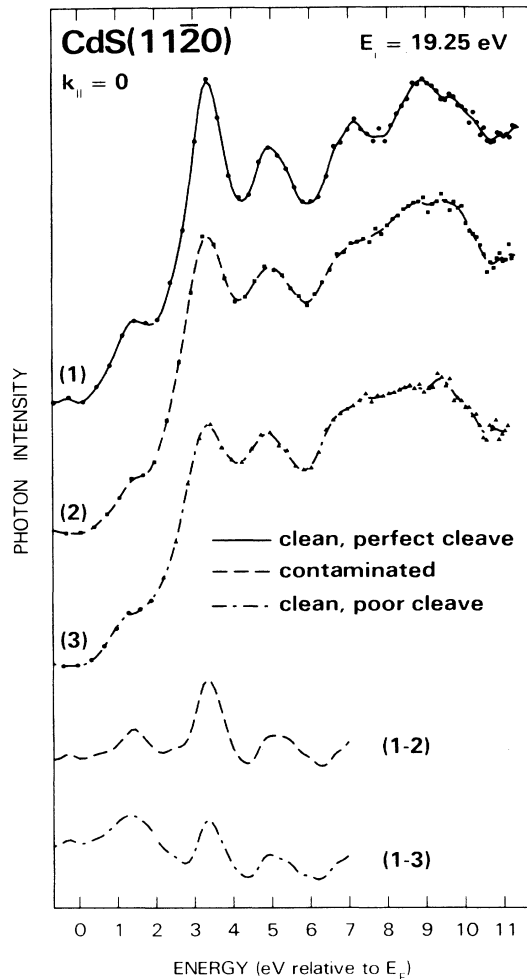


FIG. 5. Inverse photoemission spectra from CdS(11 $\bar{2}$ 0) recorded at normal incidence, $k_{\parallel} = 0$, with $E_i = 19.25$ eV. The top spectrum (1) is from a fresh cleave, spectrum (2) was recorded after contamination, and spectrum (3) is from a clean but poor cleave. The bottom curves are the difference spectra between (1) and (2) and between (1) and (3).

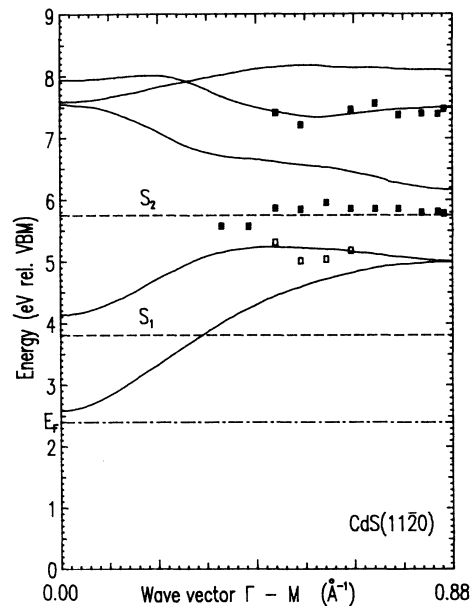


FIG. 6. Final-state energies E_f , relative to the VBM, of the transitions observed on CdS(11 $\bar{2}$ 0) plotted vs k_{\parallel} determined assuming the initial state to be free-electron-like, with a reciprocal-lattice vector $\mathbf{G} = (1,1,-2,0)$ or $(-2,-2,4,0)$. Solid squares denote conduction-band energies, open squares are weaker structures, and the surface resonances determined through contamination-dependent measurements are indicated with dashed lines. The solid lines are the calculated conduction bands from Chang *et al.* (Ref. 19) rigidly shifted to give the correct band gap for CdS. The dash-dotted line is the Fermi level.

energy position of the transition into the lowest conduction band, observed as structure *B*. The weak intensity of this structure is explained by the low transition probability into this state of mainly Cd 5s character.³⁴ We thus find the M_1 critical point at 5.8 eV above the VBM.

Left to discuss is the structure labeled *A* appearing at $E_f = 1.4$ eV above E_F , showing up as a distinct peak at low E_i and at $E_i = 19.25$ eV. The strong sensitivity of this peak to contamination and surface disorder is displayed in Fig. 5. We interpret this structure as the result of transitions into the cation- (Cd) derived unoccupied dangling-bond surface resonance on the CdS(11 $\bar{2}$ 0) UHV cleaved surface, which at $k_{\parallel} = 0$ is found 1.2 eV above the CBM. This surface resonance has also been observed in electron-energy-loss spectroscopy by Ebina *et al.*²⁴

In Fig. 5 we also observe surface sensitivity in the structure labeled *C*. In the calculation of the surface electron structure of CdTe(110) by Calandra and Santoro¹⁰ a surface feature is found splitting off the lowest conduction band at *X*. With this in mind we propose that on CdS(11 $\bar{2}$ 0) a second surface resonance is found 3.2 eV above the CBM, being split off the lowest conduction band at *M*. This conduction band is in our interpretation the dominating contribution to the structure *C*. One may notice in Fig. 5 an overall reduction of the features upon contamination and surface disorder. Our conclusions are, however, based on the relative sensitivity of the observed structures.

The structure found at a constant photon energy $h\nu = 9.25$ eV in the $E_i \geq 18.25$ -eV spectra is from the Cd 4d fluorescence process. The hole left in the Cd 4d state is filled with an electron from the VBM through a density of *p*-like states argument. With the weighted-average binding energy of the Cd 4d level of -9.5 eV,³³ the maximum in the partial density of *p* states is found 0.25 eV below the VBM.

CdSe(11 $\bar{2}$ 0)

The inverse photoemission study performed on the cleaved (11 $\bar{2}$ 0) surface of CdSe reveals information on the unoccupied bulk states which is quite analogous to what was learned above concerning this surface of CdS. However, due to experimental problems, the preparation of the surface always produced macroscopic steps. We choose therefore to defer any strong conclusions concerning surface-related features until these problems can be avoided.

In Fig. 7 the normal incidence spectra for various values of the kinetic energy of the electrons are presented. In the $E_i = 15.25$ -eV spectrum the contributions have been labeled *C'* through *E'*. Also here the fluorescent emission from transitions from the valence band into the Cd 4d level is observed at high E_i . This structure has been marked with an arrow in the $E_i = 21.25$ -eV spectrum. The emission is at a photon energy of $h\nu = 10.5$ eV, which together with the weighted average binding energy of the Cd 4d level of 10.3 eV (Ref. 35) gives the maximum in the valence partial density of *p* states 0.2 eV above the VBM. This is an indication of a Fermi-level shift on this surface as compared to the sur-

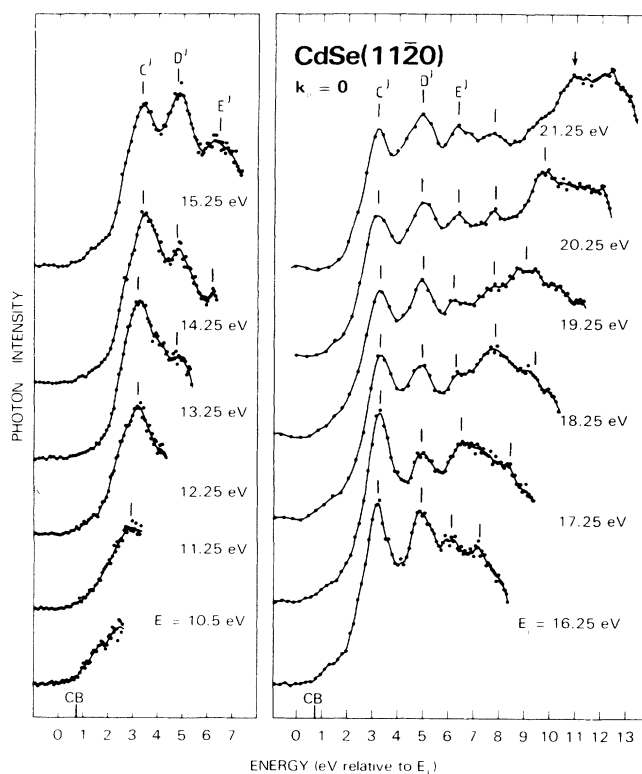


FIG. 7. Inverse photoemission spectra recorded for different kinetic energies E_i of the electrons impinging at normal incidence, $k_{\parallel} = 0$, on the cleaved (11 $\bar{2}$ 0) surface of CdSe.

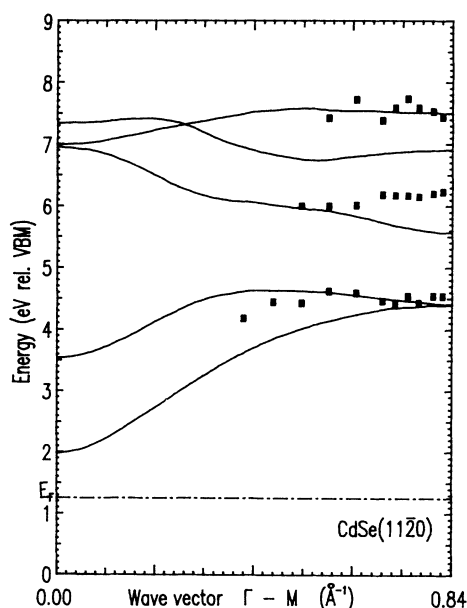


FIG. 8. Final-state energies E_f , relative to the VBM, of the transitions observed on CdSe(11 $\bar{2}$ 0) plotted vs k_{\parallel} determined assuming the initial state to be free-electron-like, with a reciprocal-lattice vector $\mathbf{G} = (1, 1, -2, 0)$ or $(-2, -2, 4, 0)$. Open squares denote weaker structures. The solid curves are the calculated conduction bands of CdS from Chang *et al.* (Ref. 19) linearly expanded to fit the larger Brillouin zone of CdSe and with the conduction bands rigidly shifted to give the correct band gap for CdSe. The dash-dotted lines is the Fermi level.

TABLE II. Summary of the critical point energies for CdTe, CdS, and CdSe found in this study. For comparison the theoretically predicted values from Chadi *et al.*, (Ref. 7), Chang *et al.* (Ref. 9), and Bergstresser and Cohen (Ref. 6) are included. The energy positions of the surface resonances found in this paper are also presented. The experimental errors are ± 0.15 eV.

	CdTe(110)		CdS(11 $\bar{2}$ 0)		CdSe(11 $\bar{2}$ 0)	
	Expt.	Chadi	Expt.	Chang	Expt.	Bergstresser
Critical-point energy (eV rel. VBM)	Γ_8 : 6.4	6.3	M_1 : 5.8	4.27	M_1 : 4.5	5.1
	X_6 : 3.7	3.85	M_4 : 7.5	6.8	M_4 : 6.3	8.0
					M_3 : 7.5	8.7
Surface resonance energy (eV rel. CBM)	S_1 : 1.4		S_1 : 1.2			
			S_2 : 3.2			

face from which the Cd 4*d* binding energy was determined. The shift is probably due to the cleavage-induced steps.

The analogs of the structures *A* and *B* found in the CdS spectra are here only observed as weak shoulders in some of the spectra.

The contributions *C'*, *D'*, *E'* are all well described within a model of direct transitions from a free-electron initial state down to the unoccupied conduction bands. The inner potential of the initial state for the transitions is taken from photoelectron spectroscopy work;³⁶ the value used is $E_0 = -4.0$ eV below the VBM. Using the photothreshold $\phi_\theta = 6.6$ eV,³² the measured work function $\Phi = 5.35$ eV, and the band gap of 1.98 eV, the Fermi energy is found to lie 0.73 eV below the conduction-band minimum. In Fig. 8 the experimental points of the conduction-band dispersions along Γ -*M* are shown together with the results of the calculation by Chang *et al.*¹⁹ for CdS. The CdS conduction bands have been linearly expanded to fit the larger Brillouin zone of CdSe and the band gap has been adjusted to that of CdSe. These two compounds are known to have very similar electronic band structures,⁶ and in this study it is clear that the experimental results have the same general character with only minor differences in energy positions. From Fig. 8 we conclude that the calculation by Chang *et al.* gives a good prediction of the conduction-band energies of CdSe, despite the fact that the calculation was performed for CdS. Table II presents the critical point energies for CdSe which have been determined in this study.

SUMMARY

Using angle-resolved inverse photoelectron spectroscopy and the statement that the observed process is the time-reversed photoemission process, we have mapped substantial parts of the conduction bands in the normal direction of cleaved CdTe(110), CdS(11 $\bar{2}$ 0), and

CdSe(11 $\bar{2}$ 0). The interpretations are based on the model of direct transitions. Under the assumption that the initial state is well approximated with a free-electron parabola, we find disagreement between experimentally observed and calculated conduction-band energies. Table II presents the experimentally determined critical-point energies together with theoretically predicted values. The experimentally determined values will hopefully stimulate further interest in the theoretical description of the electronic structure of these compounds.

We also report on the energy positions of the unoccupied surface resonances on CdTe(110) and CdS(11 $\bar{2}$ 0). The energy positions of these are presented in Table II. The cation (Cd) derived surface resonance, which for the case of the ideal CdTe(110) surface was theoretically predicted to lie ~ 0.3 eV below the conduction-band minimum at Γ ,¹⁰ is on both surfaces found well above the same. In calculations on other II-VI semiconductors¹² where the model of the surface incorporates a surface relaxation, a shift of the empty surface states into the conduction band can be found. Relaxations of this kind have also been proposed from LEED studies.¹⁵ On the CdS(11 $\bar{2}$ 0) surface a second unoccupied surface resonance is found to be split off the lowest conduction band at *M*. A similar resonance has been predicted for CdTe(110).¹⁰

Through the fluorescent emission from transitions of valence electrons into holes in the Cd 4*d* level, found in all three compounds, the energy position of the maximum in the valence partial density of *p* states is determined. This maximum is found very close to the VBM.

ACKNOWLEDGMENTS

Part of this work was supported by the Swedish Natural Science Research Council (K.O.M., U.O.K., and S.A.F.), and by a grant from the Knut and Alice Wallenberg Foundation (K.O.M.).

*Present address: MAX-lab., University of Lund, Box 118, S-221 00 Lund, Sweden.

†Present address: Mannesmann Kienzle, D-7730 VS-Villingen, Federal Republic of Germany.

‡Present address: Physics III, Royal Institute of Technology, S-100 44 Stockholm, Sweden.

¹M. Cardona and D. L. Greenaway, *Phys. Rev.* **131**, 98 (1963).

²D. T. F. Marple, *Phys. Rev.* **150**, 728 (1966).

- ³M. Cardona and G. Harbeke, *Phys. Rev.* **137**, A1467 (1964).
- ⁴M. L. Cohen and T. K. Bergstresser, *Phys. Rev.* **141**, 789 (1966).
- ⁵R. N. Euwema, T. C. Collins, D. G. Shankland, and J. S. Dewitt, *Phys. Rev.* **162**, 710 (1967).
- ⁶T. K. Bergstresser and M. L. Cohen, *Phys. Rev.* **164**, 1069 (1967).
- ⁷D. J. Chadi, J. P. Walter, M. L. Cohen, Y. Petroff, and M. Balkanski, *Phys. Rev. B* **5**, 3058 (1972).
- ⁸J. R. Chelikowsky and M. L. Cohen, *Phys. Rev. B* **14**, 556 (1976).
- ⁹See, e.g., L. Ley, R. A. Pollak, F. R. McFeely, S. P. Kowalczyk, and D. A. Shirley, *Phys. Rev. B* **9**, 600 (1974).
- ¹⁰C. Calandra and G. Santoro, *J. Vac. Sci. Technol.* **13**, 773 (1976).
- ¹¹D. H. Lee and J. D. Joannopoulos, *J. Vac. Sci. Technol.* **17**, 987 (1980); *Phys. Rev. B* **24**, 6899 (1981).
- ¹²I. Ivanov and J. Pollman, *Phys. Rev. B* **24**, 7275 (1981).
- ¹³M. F. Chung and H. E. Farnsworth, *Surf. Sci.* **22**, 93 (1970).
- ¹⁴S.-C. Chang and P. Mark, *J. Vac. Sci. Technol.* **12**, 624 (1975).
- ¹⁵C. B. Duke, A. Paton, W. K. Ford, A. Kahn, and G. Scott, *Phys. Rev. B* **24**, 3310 (1981).
- ¹⁶A. Ebina, T. Unno, Y. Suda, H. Kuoinuma, and T. Takahashi, *J. Vac. Sci. Technol.* **19**, 301 (1981).
- ¹⁷S. Takano, H. Koinuma, S. Asami, A. Ebina, and T. Takahashi, *Rec. Electron. Commun. Eng. Conversazione, Tohoku Univ.* **52**, 1 (1983); A. Ebina and Takahashi, *J. Cryst. Growth* **59**, 51 (1982).
- ¹⁸N. G. Stoffel, *Phys. Rev. B* **28**, 3306 (1983).
- ¹⁹K. J. Chang, S. Froyen, and M. L. Cohen, *Phys. Rev. B* **28**, 4736 (1983).
- ²⁰K. O. Magnusson, S. A. Flodström, P. Mårtensson, J. M. Nicholls, U. O. Karlsson, R. Engelhardt, and E. E. Koch, *Solid State Commun.* **55**, 643 (1985).
- ²¹V. Dose, *Prog. Surf. Sci.* **13**, 225 (1983); J. B. Pendry, *J. Phys. C* **14**, 1381 (1981).
- ²²F. J. Himpsel and Th. Fauster, *J. Vac. Sci. Technol. A* **2**, 815 (1984).
- ²³G. J. Lapeyre and J. Anderson, *Phys. Rev. Lett.* **35**, 117 (1975); R. S. Bauer, R. Z. Bachrach, S. A. Flodström, and J. C. McMenamin, *J. Vac. Sci. Technol.* **14**, 378 (1977).
- ²⁴A. Ebina, K. Asano, and T. Takahashi, *Phys. Rev. B* **22**, 1980 (1980).
- ²⁵D. Straub, L. Ley, and F. J. Himpsel, *Phys. Rev. Lett.* **54**, 142 (1985).
- ²⁶D. Straub, L. Ley, and F. J. Himpsel, *Phys. Rev. B* **33**, 2607 (1985).
- ²⁷D. Straub, M. Skibowski, and F. J. Himpsel, *J. Vac. Sci. Technol. A* **3**, 1484 (1985).
- ²⁸D. Straub, M. Skibowski, and F. J. Himpsel, *Phys. Rev. B* **32**, 5237 (1985).
- ²⁹W. Drube, D. Straub, and F. J. Himpsel, *Phys. Rev. B* **35**, 5563 (1987).
- ³⁰Th. Fauster, F. J. Himpsel, J. J. Donelon, and A. Marx, *Rev. Sci. Instrum.* **54**, 68 (1983); Th. Fauster, D. Straub, J. J. Donelon, D. Grimm, A. Marx, and F. J. Himpsel, *ibid.* **56**, 1212 (1985).
- ³¹F. G. Allen and G. W. Gobeli, *Phys. Rev.* **127**, 150 (1962); C. Sebenne, D. Bolomont, G. Guichard, and M. Balkanski, *Phys. Rev. B* **8**, 3280 (1975).
- ³²N. J. Shevchik, J. Tejada, M. Cardona, and D. W. Langer, *Phys. Status Solidi B* **59**, 87 (1973).
- ³³K. O. Magnusson (unpublished).
- ³⁴A. Kobayashi, O. F. Sankey, S. M. Volz, and J. D. Dow, *Phys. Rev. B* **28**, 935 (1983).
- ³⁵S. Wiklund and K. O. Magnusson (unpublished).
- ³⁶K. O. Magnusson and S. A. Flodström, *Phys. Rev. B* **35**, 2556 (1987).